Journal of Physical Education and Sport ® (JPES), Vol. 25 (issue 3), Art 49, pp. 440 - 459, March 2025
online ISSN: 2247 - 806X; p-ISSN: 2247 – 8051; ISSN - L = 2247 - 8051 © JPES

Original Article

Neurotropic effects of distilled water real exposed to Kyokushin karate katas. Neurotropic resonance: Biophotonic information transfer through Kyokushin karate katas - exposed water

VALERIY E. BABELYUK[1], IGOR L. POPOVYCH[2], OLGA SMOLEŃSKA[3], ANNA MICHALSKA[4], RADOSŁAW MUSZKIETA[5], MAGDALENA HAGNER-DERENGOWSKA[6], YURIY G. DOBROVOLSKY[7], GALYNA I. DUBKOVA[8], TETYANA A. KOROLYSHYN[9], WALERY ZUKOW[10*]
[1,2,8,9]Ukrainian Scientific Research Institute of Medicine of Transport, Odesa, UKRAINE
[2,9]Bohomolets' Institute of Physiology of NAS, Kyïv, UKRAINE
[3,4,6,10]Nicolaus Copernicus University, Torun, POLAND
[5]Merito Univeristy in Poznań, Poznań, POLAND
[7]Yuriy Fedkovych Chernivtsi National University, UKRAINE

Published online: March 31, 2025
Accepted for publication: March 15, 2025
DOI:10.7752/jpes.2025.03049

Abstract
Background. Earlier, we showed that placebo intervention (distilled water with false message of Kyokushin Karate katas, KKK, exposure) produces measurable neurotropic effects. This report presents data on neurotropic effects of water actually exposed to KKK. **Material and methods.** The study involved five male participants (aged 26-60 years, right-handed, without clinical diagnoses). In the morning, under baseline conditions, ECG recordings were taken to assess heart rate variability parameters, alongside quantitative EEG measurements at 16 loci. Then participants drank blind 30 ml of distilled water exposed to KKK by the first author. After 1.5 hours, repeated testing was performed. Control experiments were conducted with plain distilled water, well water, and filtered tap water. Baseline testing data before and after the main experiment were also used (n=70). **Results.** Preliminary analysis revealed that effects of different control waters did not differ significantly, so they were combined into one group. In the absence of spontaneous rhythmic changes (Z±SD = 0.02±0.12), enhancing informational effects were found on power spectral density of δ-rhythm in F8 locus (0.81) and index of α-rhythm (0.78) as well as right-side shift in laterality of θ-rhythm (0.37) (average: 0.65±0.25). Against weak inhibitory spontaneous changes (average: -0.22±0.15), pronounced inhibitory informational effects on 11 variables were revealed (average: -0.53±0.09). Additionally, against pronounced enhancing spontaneous changes (average: 0.35±0.17), weak inhibitory effects of KKK-treated water (-0.29±0.50) reflect significant essential inhibitory effects (average: -0.63±0.40) on 7 variables. **Conclusion.** The neurotropic effect of KKK-treated water is based on several cornerstones: ultra-weak biophoton emission from living systems, biophotons emission theory, hypothesis that photons released within the brain produce biophysical pictures during visual imagery (supported by demonstrations of increased photon emissions during white light imagination), discovery of water's fourth phase known as "EZ water" confirming "water memory" theory. When water treated with biophotons emitted during KKK enters another person, information about donor's brain activity affects recipient's brain activity and potentially the neuro-endocrine-immune network.
Keywords: **distilled water, Kyokushin Karate katas, spontaneous rhythmic changes, EEG, HRV, men**.

Introduction

Earlier, as part of the project "Functional information: Neurotropic effects of water exposed to informational factors", we showed that the placebo intervention (distilled water with the *false message* that it had been exposed to *Kyokushin Karate katas, KKK*) produces measurable neurotropic effects compared to baseline and control waters. Enhancing neurotropic Placebo effect was found on 9 variables: increase in asymmetry of δ-rhythm and its PSD in Fp2 and F4 loci, asymmetry and frequency of β-rhythm and its PSD in T3 locus, RMSSD level as well as right-side shift of laterality of δ- and α-rhythms (Z±SD = 0.92±0.66; range: 2.35÷0.26). Weak inhibitory effect (-0.23±0.06) was found on 7 variables: PSD of δ-rhythm in T6, P3 and F8 loci, θ-rhythm in Fp1 and F8 loci and α-rhythm in C4 locus as well as LFnu. Moderate inhibitory effect (-0.67±0.15) was found on 10 variables: PSD of θ-rhythm in T5, T6 and F7 loci, deviation of α-rhythm and its PSD in F8 and T5 loci, deviation of δ-rhythm and its PSD in T5 and O1 loci. Noticeable inhibitory effect (-1.14±0.27) was found on 9 variables: PSD of α-rhythm in C3, F3, T3, Fp2 and Fp1 loci, index of β-rhythm as well as HR and circulating catecholamines level. Thus, a larger number of EEG parameters are subject to the inhibitory effect of Placebo, which is accompanied by a decrease in sympathetic tone and the level of circulating catecholamines and heart rate. The sympathoinhibitory effect of Placebo was associated with inhibition of the activity of α-rhythm generating neurons and activation of δ-rhythm generating neurons as well as induction of asymmetry of δ-

Corresponding author: Walery Zukow, E-mail: w.zukow@wp.pl

rhythm. A decrease in the level of circulating catecholamines and HR was associated with the same neurotropic effects of Placebo, as well as inhibition of the activity of θ-rhythm generating neurons and asymmetry of β-rhythm. Significant individual differences in neurotropic reactions to Placebo were revealed due at least to levels of vagal tone and trait anxiety (Babelyuk et al., 2024).

This report presents data on the neurotropic effects of distilled water *really* exposed to *KKK*.

The objective of this study is to evaluate the neurotropic effects of distilled water exposed to Kyokushin Karate katas (KKK) and their impact on physiological markers, particularly quantitative EEG and HRV metrics. This research builds upon prior findings indicating that placebo-treated water produced measurable changes in neurophysiological parameters. By examining water treated with biophotonic resonance during KKK, the study aims to distinguish the effects of true informational exposure from baseline. The underlying mechanisms of water's potential to store and transmit biophysical information are also explored, with implications for understanding neural and systemic responses to biophoton-mediated influences.

The research questions addressed in this study are as follows: Does distilled water exposed to Kyokushin Karate Katas (KKK) produce measurable neurotropic effects compared to untreated distilled water? What are the mechanisms through which biophotonic resonance imparted by KKK influences neurophysiological parameters such as EEG power spectra and HRV indices?

The research hypotheses are as follows: Distilled water exposed to Kyokushin Karate Katas (KKK) induces significant and measurable neurotropic effects distinct from those of untreated distilled water; biophotonic resonance generated during KKK impacts neurophysiological activity, leading to changes in EEG power spectra and HRV indices, suggesting an interaction between water, the nervous system, and mechanisms of water memory and biophotonic information transfer.

Material and methods

Participants. The study involved five male participants (aged 26, 35, 41, 52, and 60 years, right-handed, without clinical diagnoses).

Procedure / Test protocol / Skill test trial / Measure / Instruments.

In the morning (November 16, 2010), under baseline conditions, we recorded an electrocardiogram in II lead for 7 minutes in the sitting position to assess the parameters of heart rate variability (HRV) (software and hardware complex "CardioLab+HRV" produced by "KhAI-MEDICA", Kharkiv, Ukraine). For further analyses the following HRV parameters were selected. Temporal parameters (Time Domain Methods): HR, the mode (Mo), the standard deviation of all NN intervals (SDNN), the square root of the mean of the sum of the squares of differences between adjacent NN intervals (RMSSD), the percent of interval differences of successive NN intervals greater than 50 msec (pNN_{50}); triangular index (TNN). Spectral parameters (Frequency Domain Methods): absolute ($msec^2$) and relative (%) power spectral density (PSD) bands of HRV: high-frequency (HF, range 0.4÷0.15 Hz), low-frequency (LF, range 0.15÷0.04 Hz), very low-frequency (VLF, range 0.04÷0.015 Hz), and ultralow-frequency (ULF, range 0.015÷0.003 Hz). Calculated classical indexes: LF/HF; (VLF+LF)/HF; LFnu=100%•LF/(LF+HF) (HRV, 1996; Berntson et al., 1997; Baevsky & Ivanov, 2001; Baevsky & Chernikova, 2017). Than we quantitative EEG recorded at rest a hardware-software complex “NeuroCom Standard” (KhAI MEDICA, Kharkiv, Ukraine) monopolar in 16 loci (Fp1, Fp2, F3, F4, F7, F8, C3, C4, T3, T4, P3, P4, T5, T6, O1, O2) by 10-20 international system, with the reference electrodes A and Ref on the earlobes. Two minutes after the eyes had been closed, 25 sec of artifact free EEG data were collected by computer. Among the options considered the average EEG amplitude (μV), average frequency (Hz), frequency deviation (Hz), index (%), absolute (μV^2/Hz) and relative (%) PSD of basic rhythms: β (35÷13 Hz), α (13÷8 Hz), θ (8÷4 Hz) and δ (4÷0,5 Hz) in all loci, according to the instructions of the device. In addition, we calculated coefficient of Asymmetry (As) and Laterality Index (LI) for PSD each Rhythm using equations (Newberg, 2001):

As, % = 100•(Max – Min)/Min; LI, % = Σ [200•(Right – Left)/(Right + Left)]/8 (Newberg et al., 2001).

We calculated also for HRV and each locus of EEG the Entropy (h) of normalized PSD using Popovych’s (Popadynets et al., 2020; Gozhenko et al., 2021) equations based on classic Shannon’s (1948) equation:

$$hEEG = - [PSD\alpha \cdot \log_2 PSD\alpha + PSD\beta \cdot \log_2 PSD\beta + PSD\theta \cdot \log_2 PSD\theta + PSD\delta \cdot \log_2 PSD\delta]/\log_2 4;$$

$$hHRV = - [PSDHF \cdot \log_2 PSDHF + PSDLF \cdot \log_2 PSDLF + PSDVLF \cdot \log_2 PSDVLF + PSDULF \cdot \log_2 PSDULF]/\log_2 4.$$

After completing the initial testing, participants drank blind 30 ml of Tested Water: distilled water at room temperature which had been treated by the first author as *Kyokushin karate* master (a black belt, IV Dan) (exposed to *KKK* during 4 min). Let's remind that *KKK* are generated by *imagining golden light* for 4 minutes in combination with *voluntary prolongation of exhalation*.

After 1.5 hours, repeated testing was performed.

The next day (November 18), a control experiment was conducted with the plain (untreated) distilled water, and earlier - with water from a well (November 15) and water pipe passed through a purification filter (November 10). In addition, the data of the primary testing (baseline) of the same participants, carried out both before (November 12, 11, 09, 08, October 22, 20, 10) and after (November 17, 19) the main experiment, were used (n=70).

Data collection and analysis / Statistical analysis.

Statistical processing was performed using a software package "Microsoft Excell" and "Statistica 6.4 StatSoft Inc" (Tulsa, OK, USA).

The statistical methods used for analyzing the study results included the following: 1. measures of central tendency such as mean and median to summarize the EEG and HRV parameters; 2. measures of dispersion such as standard deviation and coefficient of variation to assess variability and range for detecting outliers; 3. Z-score normalization to transform raw data for comparison against reference databases using the formula \(Z = \frac{V - N}{SD}\), where \(V\) is the raw value, \(N\) is the normal value, and \(SD\) is the standard deviation; 4. discriminant function analysis to classify EEG and HRV variables based on exposure to control waters versus KKK-treated water, calculating Wilks' Lambda and F-statistics to determine the significance of discriminant functions; 5. analysis of variance (ANOVA) to compare group means (baseline, control water, and KKK-treated water) and test for statistically significant differences among groups; 6. paired and independent t-tests to compare pre- and post-exposure data for each participant and for inter-group comparisons; 7. entropy analysis using Shannon entropy to assess the complexity and variability of normalized power spectral density (PSD) in EEG and HRV parameters; 8. cluster analysis to group EEG and HRV variables into response patterns for interpretation of combined effects; 9. chi-square tests to evaluate the distribution of categorical variables in participant responses or classification outcomes.

Results

Preliminary data analysis revealed that the effects of Control Waters (distilled, well, tap water filtered) did not differ significantly, so they were further combined into one group (CWs).

Than raw parameters were normalized by recalculation by the equations:

$Z = 4•(V – N)/(Max – Min) = (V – N)/SD = (V/N – 1)/Cv$, where

V is the raw value; N is the normal (reference) value; SD and Cv are the standard deviation and coefficient of variation respectively (Polovynko et al., 2016; Popovych et al., 2022).

Reference values are taken from the database of the Truskavetsian Scientific School of Balneology (EEG) and instruction (HRV).

As a result of the screening of the registered EEG and HRV parameters, those for which **Tested Water** significantly differs from **Baseline** and/or **Control Waters** were selected (Fig. 1).

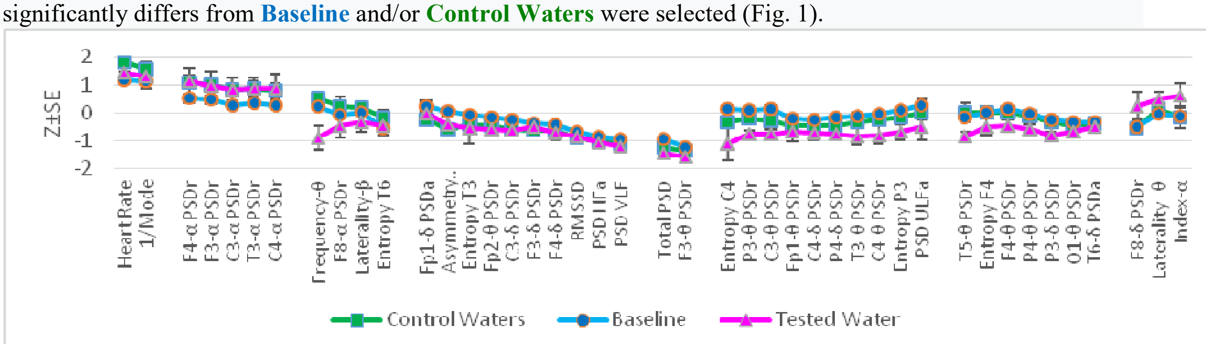

Fig. 1. Patterns of normalized EEG and HRV variables before (Baseline) and 1.5 h after consumption of 30 ml of Control Waters and distilled water treated by the author of kyokushin karate katas (Tested Water). See please also Table 5

Further, the patterns were condensed into 8 clusters, and effects of CWs (as spontaneous rhythmic changes, **SRCh}** and essential effects of *KKK* (as **Informational factor**) were also calculated (Fig. 2, details later).

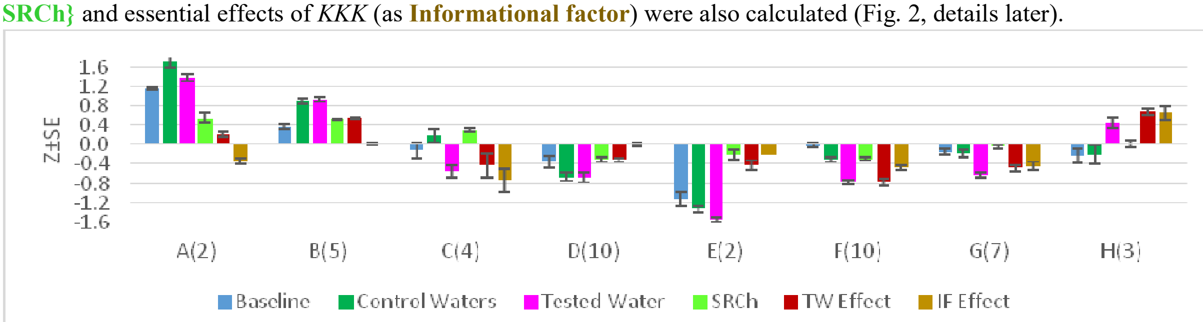

Fig. 2. Clusters of normalized EEG and HRV variables before (Baseline) and 1.5 h after consumption of 30 ml of Control Waters (CWs) and distilled water treated by the author (Tested Water, TW). See also Table 5. Calculated effects of CWs (as spontaneous rhythmic changes, **SRCh** = **CWs** - **Baseline**), **Tested Water**

Effect (**TW** - **Baseline**) and essential effects of Informational factor (**IF Effect** = **TW** - **SRCh**). The number of variables is indicated under each pattern

Following the adopted algorithm, the discriminant analysis was conducted (Klecka, 1989). First of all, it was found that only 25 variables (Tables 1 and 2) were selected by the forward stepwise program as distinguishing ones, i.e. according to the constellation of which the neural states of the participants in the basal period and 1.5 hours after the use of CWs or TW differ significantly from each other.

Table 1. Discriminant Function Analysis Summary for EEG&HRV Variables, their levels (Mean±SE) as well as Reference levels and Coefficients of Variability or SD

Step 25, N of vars in model: 25; Grouping: 3 grs; Wilks' Λ: 0,2140; approx. $F_{(50,1)}$=2,9; $p<10^{-6}$

	Groups (n)			**Parameters of Wilk's Statistics**						
Variables currently in the model	**Control Waters (15)**	**Base-line (70)**	**Tested Water B+P- (5)**	Wilks' Λ	Parti-al Λ	F-re-move (2.63)	p-level	Tole-rancy	Refe-rence (112)	Cv or **SD**
Heart Rate, bpm	85.4 3.0	80.2 1.2	82.0 3.3	0,254	0,844	5,83	0,005	0,242	70.1 0.9	0.120
RMSSD, msec	17.0 1.6	19.9 0.8	17.8 2.3	0,222	0,962	1,24	0,297	0,215	31.6 1.4	0.492
Total PSD HRV, msec²	1381 238	1658 114	1143 281	0,216	0,992	0,25	0,782	0,075	2780 108	0.411
PSD HF, msec²	114 20	154 11	110 48	0,278	0,770	9,39	10^{-3}	0,295	430 28	0.699
PSD VLF, msec²	483 86	588 46	445 89	0,224	0,954	1,51	0,228	0,141	1400 78	0,586
PSD ULF, msec²	126 30	154 21	68 50	0,225	0,951	1,64	0,203	0,255	122 10	0.883
F3-δ PSD, %	17.1 2.4	21.9 1.6	19.3 4.5	0,235	0,911	3,08	0,053	0,328	28.35 1.7	0.617
T6-δ PSD, μV²/Hz	44 11	47 7	27 7	0,225	0,951	1,61	0,208	0,443	74 8	1.110
P4-δ PSD, %	16.6 2.5	21.0 1.3	12.2 2.7	0,221	0,966	1,10	0,339	0,161	23.6 1.4	0.626
P3-δ PSD, %	19.6 3.4	21.0 1.4	11.3 2.1	0,226	0,948	1,74	0,184	0,186	25.6 1.7	0.694
Frequency-θ, Hz	7.0 0.2	6.65 0.14	5.2 0.6	0,251	0,854	5,39	0,007	0,635	6.4 0,1	0.206
Laterality-θ, %	0 6	-6.4 3.4	14 9	0,234	0,915	2,91	0,062	0,379	-5.0 3.7	SD 39
Fp1-θ PSD, %	7.5 0.6	9.2 0.5	6.1 2.0	0,228	0,939	2,05	0,137	0,317	10.4 0.6	0.588
P3-θ PSD, %	7.9 1.0	9.45 0.5	5.2 0.6	0,249	0,859	5,18	0,008	0,193	9.0 0.5	0.552
P4-θ PSD, %	8.2 0.7	8.5 0.4	6.0 0.7	0,237	0,902	3,42	0,039	0,164	8.75 0.5	0.545
Index-α, %	46 9	47 4	68 12	0,288	0,743	10,9	10^{-4}	0,146	51 2.7	0.560
F4-α PSD, %	47.6 3.7	38.9 2.3	47.9 7.2	0,228	0,938	2,07	0,134	0,057	31.1 1.4	0.485
F8-α PSD, %	34.4 5.0	29.9 2.1	23.8 6.3	0,273	0,784	8,67	10^{-3}	0,164	25.6 1.3	0.539
C3-α PSD. %	48.8 3.9	40.0 2.3	48.9 7.1	0,233	0,918	2,80	0,068	0,068	35.4 1.6	0.468
Asymmetry-β, %	13.5 1.9	23.9 2.1	16.4 4.7	0,257	0,833	6,32	0,003	0,627	23.4 1.5	0.679
Laterality-β, %	5.4 3.7	-1 3	-12 11	0,237	0,902	3,40	0,039	0,434	-1 3	SD 34
Entropy PSD F4	0.85 0.02	0.85 0.01	0.79 0.04	0,247	0,867	4,85	0,011	0,234	0.851 0.011	0.139
Entropy PSD T3	0.81 0.02	0.85 0.01	0.79 0.06	0,224	0,954	1,52	0,226	0,352	0.857 0.011	0.131
Entropy PSD C4	0.84 0.02	0.86 0.01	0.76 0.06	0,237	0,903	3,37	0,041	0,200	0.867 0.008	0.109
Entropy PSD T6	0.80 0.03	0.76 0.02	0.77 0.04	0,256	0,835	6,21	0,003	0,348	0.825 0.011	0.143

Table 2. Summary of forward stepwise analysis. Variables ranked by criterion Λ

Variables currently in the model	F to enter	p-level	Λ	F-value	p-level
Frequency-θ, Hz	4,79	0,011	0,901	4,79	0.011
Entropy PSD C4	4,18	0,019	0,821	4,46	0.002
Asymmetry-β, %	2,93	0,059	0,768	3,99	0.001
Heart Rate, bpm	3,16	0,047	0,714	3,85	10^{-3}
Entropy PSD T6	3,83	0,026	0,654	3,93	10^{-4}
PSD VLF, msec^2	2,86	0,063	0,611	3,82	10^{-4}
Index-α, %	2,63	0,078	0,574	3,70	10^{-4}
C3-α PSD. %	5,99	0,004	0,499	4,16	10^{-6}
F8-α PSD, %	2,86	0,063	0,465	4,09	10^{-6}
PSD HF, msec^2	2,87	0,063	0,434	4,05	10^{-6}
Total PSD HRV, sec^2	2,04	0,137	0,412	3,91	10^{-6}
Laterality-β, %	2,00	0,142	0,391	3,79	10^{-6}
P4-δ PSD, %	1,76	0,179	0,374	3,67	10^{-6}
P3-θ PSD, %	1,82	0,170	0,356	3,57	10^{-6}
Entropy PSD F4	2,39	0,099	0,334	3,55	10^{-6}
Fp1-θ PSD, %	2,21	0,118	0,315	3,52	10^{-6}
P4-θ PSD, %	2,90	0,061	0,291	3,56	10^{-6}
P3-δ PSD, %	1,35	0,265	0,280	3,46	10^{-6}
T6-δ PSD, μV^2/Hz	1,21	0,304	0,271	3,35	10^{-6}
F3-δ PSD, %	1,19	0,310	0,262	3,25	10^{-6}
F4-α PSD, %	1,59	0,211	0,250	3,19	10^{-6}
Laterality-θ, %	1,52	0,227	0,239	3,14	10^{-6}
Entropy PSD T3	1,27	0,288	0,230	3,07	10^{-6}
PSD ULF, msec^2	1,06	0,353	0,222	2,99	10^{-6}
RMSSD, msec	1,24	0,297	0,214	2,93	10^{-6}

The rest of the variables were outside the discriminant model, probably due to duplication or redundancy of identifying information.

Table 3. Discriminant Function Analysis Summary for EEG&HRV Variables currently not in the Model

Variables	Groups (n)			Parameters of Wilk's Statistics						
	Control Waters (15)	**Base-line (70)**	**Tested Water B+P- (5)**	Wilks' Λ	Parti-al Λ	F to enter	p-level	Tole-rancy	Refe-rence (112)	Cv
Mode HRV, msec	699 26	742 14	725 40	0,212	0,991	0,27	0,761	0,165	855 9	0.117
Fp1-δ PSD, μV^2/Hz	41 8	73 13	54 26	0,210	0,980	0,62	0,540	0,487	58 6	1.132
F4-δ PSD, %	18.5 2.0	22.7 1.5	17.2 5.4	0,211	0,985	0,48	0,621	0,102	31.2 1.3	0.624
F8-δ PSD, %	22.0 3.9	23.3 2.1	40.7 11	0,212	0,989	0,34	0,712	0,283	35.2 2.2	0.656
C3-δ PSD, %	18.1 2.8	23.4 1.5	17.1 3.9	0,214	0,998	0,05	0,951	0,120	28.0 1.6	0.602
C4-δ PSD, %	19.8 2.9	23.9 1.4	15.4 4.2	0,213	0,993	0,21	0,808	0,125	28.2 1.6	0.613
Fp2-θ PSD, %	7.1 0.7	8.9 0.5	6.3 1.8	0,211	0,988	0,37	0,695	0,344	9.9 0.6	0.620
F3-θ PSD, %	10.2 1.1	12.0 0.6	7.2 1.0	0,210	0,981	0,61	0,546	0,164	31.1 1.4	0.485
F4-θ PSD, %	11.1 1.2	11.8 0.6	8.3 1.3	0,214	0,998	0,05	0,954	0,163	11.1 0.6	0.539
T3-θ PSD, %	8.7 1.0	9.8 0.5	6.3 1.5	0,212	0,992	0,24	0,790	0,215	10.3 0.5	0.466
C3-θ PSD, %	9.7 0.8	11.8 0.6	7.4 0.8	0,213	0,997	0,09	0,910	0,152	11.1 0.4	0.424
C4-θ PSD, %	9.8 0.7	10.9 0.4	7.3 1.6	0,213	0,997	0,08	0,923	0,248	11.1 0.4	0.422
T5-θ PSD, %	9.7 1.5	9.0 0.5	5.8 0.7	0,208	0,974	0,82	0,446	0,311	9.7 0.4	0.471
O1-θ PSD, %	5.9 0.7	6.5 0.5	5.0 0.6	0,212	0,991	0,28	0,755	0,365	8.2 0.5	0.584
F3-α PSD, %	48.8 3.7	40.4 2.3	48.4 8.0	0,211	0,988	0,37	0,692	0,022	33.2 1.5	0.479

T3-α PSD, %	43.2 3.8	35.5 2.0	43.3 5.8	0,211	0,988	0,38	0,680	0,075	30.4 1.4	0.483
C4-α PSD, %	46.3 4.0	38.9 2.3	47.6 7.7	0,210	0,983	0,54	0,585	0,038	34.8 1.4	0.432
Entropy PSD P3	0.78 0.03	0.81 0.01	0.71 0.94	0,213	0,997	0,10	0,902	0,128	0.802 0.013	0.167

The identifying information contained in the 25 discriminant variables is condensed into two roots. The major root contains 64.7% of discriminatory opportunities (r*=0.779; Wilks' Λ=0.214; $\chi^2_{(50)}=116$; $p<10^{-6}$), minor root 35.3% (r*=0.676; Wilks' Λ=0.544; $\chi^2_{(24)}=46$; p=0.005).

The next goal of discriminant analysis is visualization of each participant in the information space of roots (Fig. 3). It is achieved by calculating the values of discriminant roots for each person by the raw coefficients and the constants (Table 4).

Table 4. Standardized and raw coefficients and constants for discriminant EEG variables

Coefficients	**Standardized**		**Raw**	
Variables	Root 1	Root 2	Root 1	Root 2
Frequency-θ, Hz	-0,303	0,618	-0,263	0,537
Entropy PSD C4	0,862	0,267	9,325	2,888
Asymmetry-β, %	0,639	0,205	0,039	0,013
Heart Rate, bpm	-0,863	0,654	-0,082	0,063
Entropy PSD T6	-0,851	-0,277	-6,763	-2,203
PSD VLF, msec^2	0,692	-0,278	0,002	-0,001
Index-α, %	1,701	0,170	0,048	0,005
C3-α PSD. %	-1,397	-0,199	-0,076	-0,011
F8-α PSD, %	-0,799	1,427	-0,045	0,080
PSD HF, msec^2	-1,094	0,342	-0,006	0,002
Total PSD HRV, msec^2	-0,412	0,027	-0,0004	0,00003
Laterality-β, %	-0,570	0,246	-0,023	0,010
P4-δ PSD, %	0,013	0,677	0,001	0,065
P3-θ PSD, %	1,098	0,002	0,259	0,0005
Entropy PSD F4	-0,922	0,348	-8,536	3,228
Fp1-θ PSD, %	0,554	0,120	0,144	0,031
P4-θ PSD, %	-0,991	-0,016	-0,333	-0,005
P3-δ PSD, %	-0,682	0,003	-0,059	0,0003
T6-δ PSD, μV^2/Hz	0,412	0,121	0,008	0,002
F3-δ PSD, %	-0,278	-0,702	-0,022	-0,054
F4-α PSD, %	-0,511	-1,422	-0,028	-0,078
Laterality-θ, %	0,275	-0,623	0,010	-0,022
Entropy PSD T3	0,372	-0,321	4,172	-3,596
PSD ULF, msec^2	0,006	0,652	0,00003	0,004
RMSSD, msec	-0,264	0,542	-0,042	0,086
	Constants		16,00	-11,83
	Eigenvalues		1,540	0,840
Cumulative Proportions			0,647	1

Following the previous approach, we still included in Table 5 17 variables that were not included in the discriminant model, since they organically fit into the factorial structure of the roots.

Table 5. Correlations between variables and roots; centroids of clusters, and Z-scores

Variables	**Correlations Variables-Roots**		**Control Waters (15)**	**Baseline (70)**	**Tested Water B+P- (5)**	**Clu-sters (Figs. 1&2)**
Root 1 (64.7%)	**Root 1**	**Root 2**	**-2.72**	0.51	0.96	
Heart Rate	**-0,146**	-0,060	**1,84±0,37**	1,19±0,14	1,45±0,41	**A**
1/Mode HRV			**1,57±0,25**	1,13±0,13	1,30±0,42	**A**
F4-α PSDr	**-0,126**	-0,139	**1,09±0,24**	0,52±0,15	1,12±0,48	**B**
F3-α PSDr			**0,98±0,23**	0,46±0,14	0,96±0,51	**B**
C3-α PSDr	**-0,128**	-0,137	**0,81±0,24**	0,28±0,14	0,82±0,43	**B**
T3-α PSDr			**0,87±0,26**	0,34±0,14	0,88±0,40	**B**
C4-α PSDr			**0,77±0,26**	0,28±0,15	0,85±0,52	**B**
Frequency-θ	**-0,147**	0,303	**0,51±0,18**	0,21±0,11	-0,89±0,44	**C**
F8-α PSDr	**-0,090**	0,076	**0,22±0,33**	-0,08±0,14	-0,48±0,42	**C**
Laterality-β	**-0,098**	0,102	**0,18±0,11**	-0,01±0,09	-0,34±0,34	**C**
Entropy PSD T6	**-0,116**	-0,035	**-0,16±0,23**	-0,57±0,13	-0,48±0,32	**C**
Root 2 (35.3%)	**Root 1**	**Root 2**	-0.17	**0.30**	**-3.65**	

Fp1-δ PSDa			-0,26±0,13	0,23±0,20	-0,06±0,39	D
Asymmetry-β	0,177	0,137	-0,62±0,12	0,03±0,13	-0,44±0,30	D
Entropy PSD T3	0,102	0,162	-0,42±0,21	-0,10±0,09	-0,57±0,54	D
Fp2-θ PSDr			-0,46±0,11	-0,17±0,08	-0,59±0,29	D
C3-δ PSDr			-0,59±0,17	-0,27±0,09	-0,65±0,23	D
F3-δ PSDr	0,106	0,063	-0,64±0,14	-0,37±0,09	-0,52±0,26	D
F4-δ PSDr			-0,65±0,10	-0,44±0,08	-0,72±0,28	D
RMSSD	0,128	0,099	-0,90±0,10	-0,69±0,06	-0,85±0,11	D
PSD HFa	-0,021	0,128	-1,05±0,05	-0,88±0,06	-1,09±0,09	D
PSD VLF	0,080	0,115	-1,13±0,11	-0,95±0,06	-1,19±0,06	D
Total PSD HRV	0,070	0,148	-1,27±0,17	-0,96±0,10	-1,48±0,06	E
F3-θ PSDr			-1,38±0,08	-1,27±0,04	-1,59±0,07	E
Entropy PSD C4	0,030	0,258	-0,34±0,23	0,13±0,12	-1,11±0,63	F
P3-θ PSDr	0,073	0,263	-0,21±0,19	0,09±0,11	-0,76±0,13	F
C3-θ PSDr			-0,30±0,17	0,14±0,12	-0,79±0,17	F
Fp1-θ PSDr	0,105	0,213	-0,47±0,10	-0,20±0,08	-0,70±0,33	F
C4-δ PSDr			-0,48±0,17	-0,25±0,08	-0,74±0,25	F
P4-δ PSDr	0,097	0,225	-0,47±0,17	-0,18±0,09	-0,77±0,18	F
T3-θ PSDr			-0,34±0,21	-0,11±0,10	-0,84±0,31	F
C4-θ PSDr			-0,27±0,16	-0,05±0,09	-0,81±0,33	F
Entropy PSD P3			-0,16±0,26	0,07±0,11	-0,69±0,28	F
PSD ULFa	0,034	0,135	0,02±0,27	0,27±0,19	-0,53±0,46	F
T5-θ PSDr			-0,01±0,34	-0,15±0,11	-0,85±0,15	G
Entropy PSD F4	-0,023	0,133	0,00±0,20	-0,01±0,11	-0,50±0,33	G
F4-θ PSDr			0,01±0,20	0,12±0,10	-0,46±0,22	G
P4-θ PSDr	0,003	0,215	-0,12±0,15	-0,05±0,08	-0,58±0,14	G
P3-δ PSDr	0,006	0,215	-0,34±0,19	-0,26±0,08	-0,80±0,12	G
O1-θ PSDr			-0,48±0,14	-0,35±0,10	-0,67±0,13	G
T6-δ PSDa	0,008	0,094	-0,37±0,14	-0,32±0,08	-0,53±0,09	G
Laterality- θr	-0,040	-0,190	0,12±0,16	-0,04±0,09	0,49±0,24	H
Index-α	0,030	-0,149	-0,17±0,39	-0,13±0,15	0,61±0,44	H
F8-δ PSDr			-0,57±0,17	-0,51±0,08	0,24±0,49	H

The displacement of localization along the axis of the major root of the cluster of CWs relative to the basal cluster (Fig. 3) reflects the enhancing of the variables associated with the root positively (clusters A, B, C; see also Figs. 1 and 2).

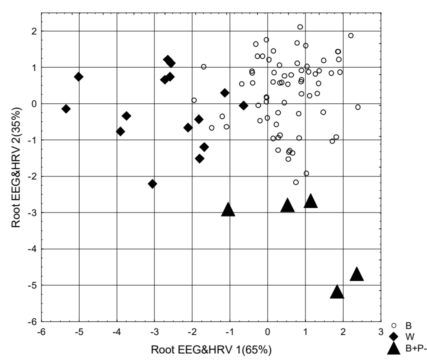

Fig. 3. Scattering of individual values of discriminant roots before (B) and 1.5 h after consumption of 30 ml of control waters (well, distilled, tap water filtered) (W) and blind 30 ml of distilled water treated by the Babelyuk (B+P-) by using Kyokushin karate katas

At the same time, the projections on the axis of individual roots after the use of the Tested Water. are mixed with the projections of the basal cluster, which reflects the absence of changes in these same variables.

Instead, the Tested Water cluster is shifted relative to the basal cluster along the minor root axis, which reflects the inhibition of the variables associated with it positively (clusters D, E, F, G) while the enhancing of three variables associated with root negatively (cluster H).

Despite some mixing, the demarcation of three clusters in the information space of two roots is highly reliable (Table 6).

Table 6. Squares of Mahalanobis distances between groups (above the diagonal) and F-criteria (df=25.6) as well as p-levels (below the diagonal)

Groups	Baseline (70)	Control Waters (15)	Tested Water B+P- (5)
Baseline	0	10.7	15.7
Control Waters	3,82 10^{-5}	0	25.6
Tested Water	2.13 0,008	2,79 0.001	0

Another consequence of discriminant analysis is the possibility to retrospectively identify one or another state of each participant: basal and after drinking control or tested water. This goal of discriminant analysis is realized with the help of coefficients and constants of classification functions (Table 7).

Coefficients and constants of classification functions.

It is important that the state after consumption of KKK-treated water is classified without error, despite the small number of tests (Table 7). We explain the two errors in cases of CWs use by the absence of spontaneous rhythmic changes, as well as the excess of the latter in the two basal states.

Table 7. Classification matrix. Rows: Observed classification; Colums: Predicted classification

Group	% correct	Baseline p=0,778	CWs p=0,167	KKK-W p=0,055
Baseline	97,1	68	2	0
Control Waters	86,7	2	13	0
KKK-treated Water	100	0	0	5
Total	95,6	70	15	5

Discussion

The information presented in Figs. 1 and 2, was later reformatted in such a way as to put Functional Information Effects and their ranking in the foreground (Figs. 4 and 5). In the absence of SRCh (Z±SD = 0.02±0.12; the first on the right) an enhancing in Informational effects on PSD of δ-rhythm in F8 locus (0.81) and index of α-rhythm (0.78) as well as right-side shift in laterality of θ-rhythm (0.37) was found (average: 0.65±0.25). Against the background of weak inhibitory SRCh (average: -0.22±0.15; the second on the left), pronounced inhibitory Informational effects on PSD of θ-rhythm in P3 (-0.55), C4 (-0.54), T3 (-0.50), C3 (-0.49), F4 (-0.47), P4 (-0.46) loci, PSD of δ-rhythm in P3 locus (-0.46), entropy of PSD in C4 (-0.77), P3 (-0.55), F4 (-0.47) loci as well as PSD of ULF band HRV (-0.55) were revealed (average: -0.53±0.09). In addition, against the background of pronounced enhancing SRCh (average: 0.35±0.17; the first on the left), the weak inhibitory effects of the tested water (-0.29±0.50) reflect the significant *essential* inhibitory effects (average: -0.63±0.40) of the Information that this water carries, on frequency of θ-rhythm (-1.40) and its PSD in T5 (-0.84) locus, PSD of α-rhythm in F8 (-0.70) locus, entropy of PSD in T6 (-0.32) locus, heart rate (-0.39) and 1/Mode HRV (-0.27) as marker of circulating catecholamines as well as left-side shift in laterality of β-rhythm (-0.52). In the rest of the clusters, the essential Informational effects are scarce or completely absent (the fifth cluster), since the effects of KKK-treated water differ little or not at all from spontaneous rhythmic changes.

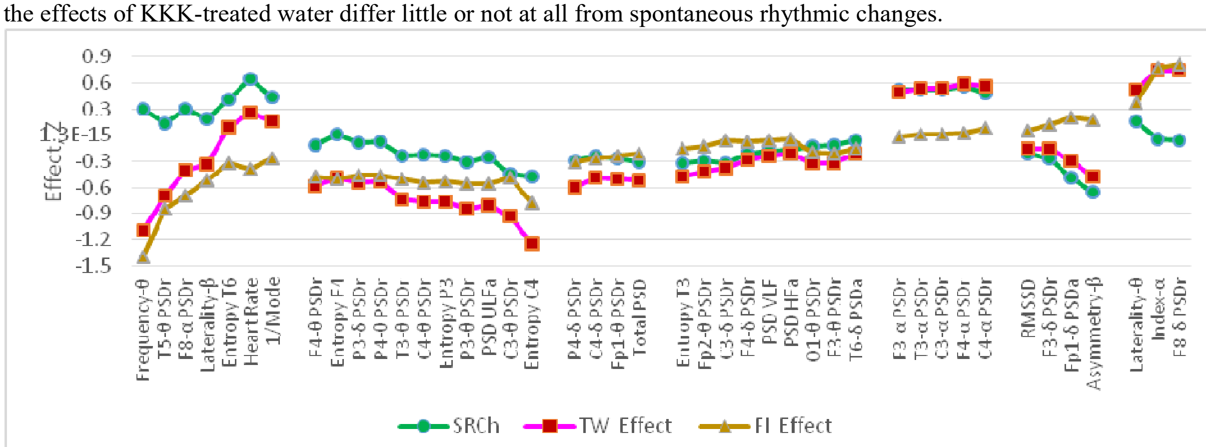

Fig. 4. Profiles of neurotropic Functional Information Effects and accompanied effects of Tested Water (TW) as well as spontaneous rhythmic changes (SRCh).

Spontaneous rhythmic changes calculated by equation: SRCh = CWs – Baseline; TW Effect = TW – Baseline; FI Effects = TW Effects - SRCh = TW CWs

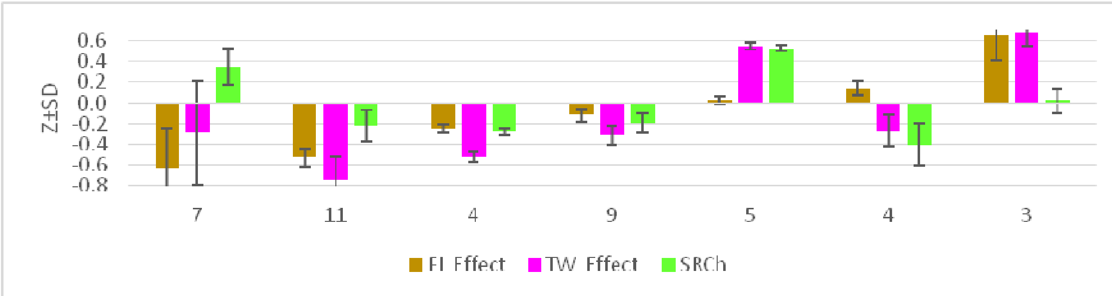

Fig. 5. The clusters of inhibitory, neutral and enhancing neurotropic Functional Information Effects and accompanied effects of Tested Water (TW) as well as spontaneous rhythmic changes (SRCh).
Spontaneous rhythmic changes calculated by equation: SRCh = CWs – Baseline; TW Effect = TW – Baseline; FI Effects = TW Effects - SRCh

When considering individual neurotropic reactions (Fig. 6), firstly, 3 moderate and 2 severe responders were found; secondly, more pronounced SRCh in participant Ly than other participants. Participants Ly and Kh also demonstrated the group's maximum sensitivity to the information effect of KK-treated water (Fig. 7). Elucidation of predictors of such features will be carried out in the next article.

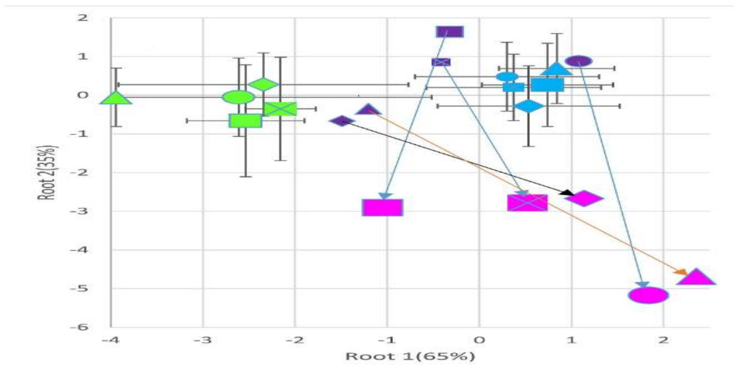

Fig. 6. Scattering of individual values of discriminant roots before and 1.5 h after consumption of 30 ml of distilled water treated by the Babelyuk, as well as control waters (Mean±SD, n=3). The mean baseline (M±SD, n=9 - 16) of each recipient are shown (Kh circle, Ba rhombus, Ly triangle, Le square, Sh square with diagonals)

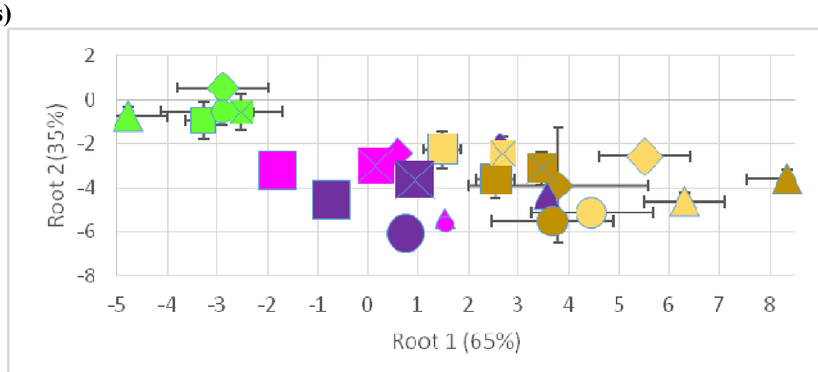

Fig. 7. Scattering of individual changes in discriminant roots 1.5 h after consumption of 30 ml of distilled water treated by the Babelyuk, and Control waters (Mean±SE, n=3). Individual essential Functional Information effects calculated as differences between changes in discriminant roots 1.5 h after consumption of Tested water and Control waters. ***The calculation was carried out separately for the basal variables in this experiment and the entire series. The markers of the recipients: Kh circle, Ba rhombus, Ly triangle, Le square, Sh square with diagonals***

So, the neurotropic effect of *KKK*-treated water is a proven fact (we will look forward to the counterarguments of the skeptics, remembering the lifetime compromise and posthumous universal recognition of such geniuses as Gurwitsch and Benveniste).

This phenomenon is based on several cornerstones, the first of which is the **ultra-weak glow of living systems**, discovered by Gurwitsch back in 1922 at the University of Tavria (Simferopol, Ukraine) and called by him "mitogenetic radiation" (Gurwitsch, 1926; 1945; 1959; Beloussov et al., 1997) which attracted worldwide attention in the 1920s and 1930s, but was largely forgotten and partially compromised.

Popp's (1979-2003) and Van Wijk's (1992-2008) laboratories revived this line of research, introduced the term "biophotons", in their laboratories devices were created for biophotons registration - analogue photomultiplier tubes (PMT). Researchers showed that living systems emit in the order of 10^6 photons per m^2 s (Popp, 1979; Cohen & Popp, 1997; Van Wijk et al., 2006). Assuming an average wavelength of 500 nm (0.6 petaHz), the energy (the product of the frequency of the electromagnetic wave and Planck's constant) would be □4×10^{-19} J for a sum of about 4×10^{-13} W/m^2 (Dotta et al, 2012). This value is just above the background energy densities (□10^{-13} W/m^2) for cosmic rays near the Earth's surface and that produced from natural radioactive isotopes from the atmosphere and ground (Koenig et al., 1981). The value of 10^{-20} J is congruent with the energy between the individual ions (potassium) that are most correlated with the resting membrane potential of cells (Persinger, 2010). In addition, the effect of a single action potential (net change of 1.2×10^{-1} V) upon a unit charge (1.6×10^{-19} A s) is about 2×10^{-20} J. This "quantum" of energy is also the amount required to stack a nucleotide on a synthesizing RNA sequence as well as other essential biophysical parameters (Persinger, 2010).

Popp et al. (1984) proved that the source of biophotons emission is DNA. Dotta et al. (2011) showed that photon emissions from depolarizing cell cultures were primarily emitted from the plasma membrane. The main source of biophotons derives from the oxidative metabolism of mitochondria (Kataoka et al., 2001). Neurons also incessantly emit biophotons. Biophoton emission from neural tissue depends on the neuronal membrane depolarization and Ca^{2+} entry into the cells (Kataoka et al., 2001).

Kobayashi et al (1999; 1999a) found that baseline photon emissions from rat brains were between $\sim10^{-11}$ and 10^{-12} W/m^2. The value decreased by about 60% of baseline levels following a protracted period of hypoxia. During hyperoxia (100% O_2 inhalation) photon emission intensity was enhanced by 130% relative to baseline particularly over the frontal regions. Theta wave power within slices of hippocampus was coupled to the intensity of the photon emissions

Bókkon (2009) proposed a redox molecular hypothesis about the natural biophysical substrate of visual perception and visual imagery. This hypothesis is based on the redox and bioluminescent processes of neuronal cells in retinotopically organized cytochrome oxidase-rich **visual areas**. This hypothesis is in line with the functional roles of reactive oxygen and nitrogen species in living cells that are not part of a haphazard process, but rather a very strict mechanism used in signaling pathways. Author point out that there is a direct relationship between **neuronal activity and the biophoton emission process in the brain**. Electrical and biochemical processes in the brain represent sensory information from the external world. During encoding or retrieval of information, electrical signals of **neurons** can be converted into synchronized **biophoton** signals by bioluminescent radical and non-radical processes. Therefore, information in the brain appears not only as an electrical (chemical) signal but also as a regulated biophoton (weak optical) signal inside neurons. During visual perception, the topological distribution of photon stimuli on the retina is represented by electrical neuronal activity in retinotopically organized visual areas. These retinotopic electrical signals in visual neurons can be converted into synchronized biophoton signals by radical and non-radical processes in retinotopically organized mitochondrial-rich areas. As a result, regulated bioluminescent biophotons can create intrinsic pictures (depictive representation) in retinotopically organized cytochrome oxidase-rich visual areas during **visual imagery** and visual perception. The long-term visual memory is interpreted as epigenetic information regulated by free radicals and redox processes. This hypothesis does not claim to solve the secret of consciousness, but proposes that the evolution of higher levels of complexity made the intrinsic picture representation of the external visual world possible by regulated redox and bioluminescent reactions in the visual system during visual perception and **visual imagery**.

Rahnama, Bókkon et al. (2011) argued that, in addition to electrical and chemical signals propagating in the neurons of the brain, signal propagation takes place in the form of biophotons production. This statement is supported by recent experimental confirmation of photon guiding properties of a single neuron. The authors have investigated the interaction of mitochondrial biophotons with microtubules from a quantum mechanical point of view. Their theoretical analysis indicates that the interaction of biophotons and microtubules causes transitions/fluctuations of microtubules between coherent and incoherent states. The authors argued that the role of biophotons in the brain merits special attention.

To test Bókkon's hypothesis, four separate studies were conducted in the Persinger's laboratory (Hunter et al, 2010; Dotta et al, 2012; Saroka et al, 2013; Persinger et al., 2013).

The first experiment (Hunter et al, 2010) with a psychic Sean Harribance demonstrated an increase of photon emission from his right hemisphere when he was "calling his angel" - engaged in the "interpretational state". The authors found a significant inverse correlation between the intensity of photon emission and intensity of the horizontal geomagnetic field (perpendicular to the temporal plane). Decreases over 10 to 15 s of 15 nT and 5 nT at 0,25 m and 1 m from the right side of his head were associated with the same magnitude of energy (10^{-11} J) that was associated with the net increase in photon emissions during that period. This energy, assuming each action potential is associated with $1{,}9\cdot10^{-20}$ J, would be the equivalent of the activity of about 1 billion neurons (the human cerebral cortices contain in the order of 20 to 40 billion of neurons). Such visual imagery accompanied by activation of certain areas of the brain.

The second study (Dotta et al., 2012) was conducted with the participation of 8 **normal** volunteers (ages 23 through 26; 4 men, 4 women). In the first experiment, the authors measured the photon emission from the right side of the head in the same plane as the temporoparietal lobes. Instructions to think about white light (60 s) and project the light into the PMT along the right side of the head followed rest or "baseline" intervals (also 60 s, most of which involved either no recollection or thoughts about friends or studies) were given vocally from another room and repeated three times. The means for the PMT values for each of the 6 intervals (3 thinking about light, 3 not) were obtained for each subject. There was a statistically significant increase in ultraweek photon emission (UPE) while the subjects were thinking about white light compared to not thinking about light. This increase was noted for all 8 subjects. The net difference in energy emission between the two conditions ranged between 25 and 100 pW/m^2. In general, from the time of the instruction to imagine white light to the first increases in photon emission above background fluctuations was about 4 s. During the 60 s intervals of imaging white light the durations of the elevations in UPE occurred in cycles of approximately 7–9 s peaks followed by 3–4 s troughs. This was not observed during the intervals of the reference condition. These fluctuations suggest that the averaged values for the UPE per 60 s interval may be underestimates of the peak output. During the PMT measurements for the same instruction procedure in the second experiment (QEEG) was recorded 3 subjects. The correlation between the average fluctuations in quantitative EEG power (sum of all bands) over the left prefrontal region for the intervals of "imaging light" and the fluctuations in UPE from the right hemisphere was 0.95.

On the other hand, the energy for photon emissions was negatively correlated with the power within the beta band (13–20 Hz) over the right frontal (rho and $r = -0.65$, $p<0.05$) lobe with marginal effects over the right temporal lobe (T4, $r = -0.40$, $p<0.10$). There was no significant correlation ($r = 0.13$, $p>0.05$) between the energy of biophoton emission from the right hemisphere and the EEG power over the left prefrontal region during the intervals associated with not thinking about white light, i.e., thoughts about mundane events.

At a distance of 0.15 m for this system, where 1 unit increase is 5×10^{-11} W/m^2, the increased photon emission while thinking of white light would be equivalent to between 3 and 6×10^{-12} J/s when the cross-sectional area of the cerebrum is accommodated. When divided by the essential quantum of 2×10^{-20} J/action potential (Persinger, 2010) and assuming an average of □20 Hz per neuron, this would suggest that an additional 10^7 (on average) neurons within the cerebral cortices were activated during the imagining of light by the subjects. One argument that the photon emissions were functionally coupled to cognition was the strong correlation between the power spectra of the quantitative EEG during intervals when the light was being visualized and the absolute increase in UPE. The net change in EEG power associated with the range in photon density while imagining white light (vs. not imagining) was □25 $\mu V^2/Hz$. When this value is multiplied by the sum of 1 Hz increments within about 15 Hz (low beta band) the potential is 20 μV. The net change in energy detected by the PMT during this activity was □2×10^{-9} W/m^2 or 3×10^{-10} J from the cerebrum at the measured distance. The quotient of energy to voltage would be □10^{-5} A s or the equivalent of 10^{14} charges. With the summed movement of about 10^6 to 10^7 ions across a membrane (Persinger, 2010) to produce an action potential, this would involve about 10^7 to 10^8 neurons. A particularly intriguing observation was the strong positive correlation between EEG power from the left prefrontal region and UPE from the right side of the head but negative correlation between frontal and temporal EEG power (within the beta range) over the right hemisphere and UPE. The left prefrontal positive correlation is consistent with the volitional and intentional nature of the task. However, this inverse relationship between cerebral fluctuation in electroencephalographic voltage and photon levels from the right hemisphere would be consistent with the principle of conservation of energy.

The third study (Saroka et al., 2013) was conducted with the participation of 2 normal volunteers (non-meditators) and one meditator. Is was shown, that the real time absolute values of the correlations between photon emissions and electroencephalographic power were moderately strong and indicated that the fluctuations in amplitudes of photon emissions and the ratio of alpha/beta activity shared about 25% of the variance. This association was found primarily between whole right hemispheric photon emission and the electroencephalographic power within a specific region of the brains: the right prefrontal-central areas. However, it is noteworthy that a decrease in photon emissions was also recorded, more pronounced in both non-meditators, and moreover, with the same magnitudes of the correlation coefficients, their signs were opposite. The results of the coupled, real-time measurements of the changes in the Earth's magnetic field intensity at 25 cm from the right side of the meditator's head and concurrent photon emission were similar to the measurements of Sean Harribance (Hunter et al., 2010) while he focused upon the "inner light" during which time he reported information about others. The slope of the equation indicated that for every $0.5\cdot10^{-11}$ W/m^2 increase in photon emissions from the subject's right hemisphere there was 10 nT decrease in the intensity of the Earth's magnetic field in the horizontal plane.

The subject of fourth experiment (Persinger et al., 2013) was a 28 years old female graduate student in Psychology. She has been a meditation practitioner for approximately 5 years and a Level II Reiki practitioner for two years. She was asked to think about sending light out from her consciousness into the sensor of the PMT for about 2 min which was followed by 2 min of relaxation. The procedure was repeated four times with a rest of about 5 minutes between the 2 min-2 min pairs in order to reset some of the equipment (from outside of the chamber). The numbers of photons were sampled 50 times per second (20 ms Δt) while the EEG data from all sensors were sampled at 250 times per second. The geomagnetic field measures were sampled 3 times per second. The differences in collection times were limited by the software associated with the different equipment. Authors selected 2 min sequences for measurement rather than 30 s, employed in previous studies, to ensure time for the cognitive processes to maximally affect the photon emissions.

There was marked increased in power within the delta (1 to 4 Hz) band and the low beta to gamma band (13 to 35 Hz) associated with bilateral activation within the parahippocampal gyri within both hemispheres during periods when light was imagined compared to the non-imagining intervals (rest periods). Oneway analysis of variance indicated there was significantly more power within this band during the imagining compared to the "non imagining" periods. **Only during the first 15 s of each of the 4 trials where white light was imagined was the photon emission significantly higher** than the equivalent first 15 s of the resting trials.

The correlation (r, rho) between the change (in nT) for the horizontal component of the geomagnetic field and the numbers of photon counts for the 2 min intervals was strongly negative (-0.90, -0.83, respectively). This effect was similar to what the authors have measured in two previous studies (Hunter et al., 2010; Saroka et al., 2013). The decrease in the change of the intensity in the geomagnetic field was clearly associated with an increased cerebral photon emission. The mean decrease in range during the intervals of imagining white light was about 7 nT (Persinger et al., 2013).

Rubik & Jabs (2017) conducted a unique experiment involving a 54-year-old male. Hi is a highly experienced practitioner and teacher from the International Academy of Consciousness (IAC). The IAC develops and teaches techniques that help people achieve out-of-the-body states to explore the multidimensionality of consciousness. One technique is the Voluntary Energetic Longitudinal Oscillation (VELO). To perform VELO, one continuously mobilizes an energetic pulse in complete, successive, longitudinal cycles up and down the whole body length, with the objective of producing a cohesive, stationary wave that encompasses the entire energetic body. Induction of the VELO may lead to the vibrational state, considered by the IAC one of the most fundamental resources of lucid psychic self-control. In this case study, the subject was first measured in his ordinary state of consciousness and then while performing VELO. Measurements were made for two minutes at each bodily region alternating with baseline measurements as previously described. The raw data from the PMT are shown in Fig. 8.

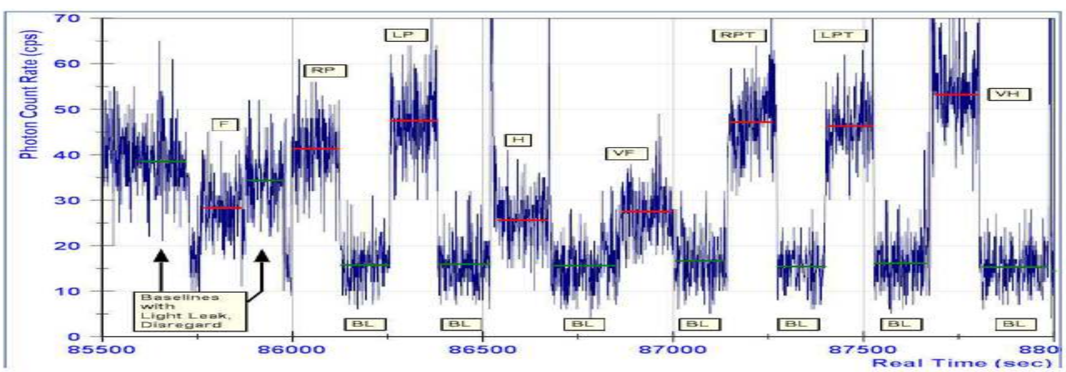

Fig. 8. Session with Subject 5 showing biophoton emission in cps. BL=baseline; F=forehead; RP=right palm; LP=left palm; H=heart; VF=forehead during VELO; RPT=right palm transmitting energy during VELO; LPT=left palm transmitting energy during VELO; VH=heart during VELO (Rubik & Jabs, 2017).

Alternative, if not surrogate, but much cheaper methods of assessing biophoton emission are methods based on the Kirlian effect (Kilrian, 1949; Kirlian & Kirlian, 1961).

The method of *Colour coronal spectral analysis* on a device with an electrode made of polyethylene terephthalate with applied electric voltage 15 kV, electric impulse duration 10 µs, and electric current frequency 15 kHz detected the specific photon emission from part of the human thumb as a spectrum of various colours (Ignatov & Mosin, 2016). It was established that photons corresponding to a red color emission of visible electromagnetic spectrum have energy at 1.82 eV. The orange color - 2.05, yellow – 2.14, blue-green (cyan) – 2.43, blue – 2.64, and violet – 3.03 eV. The reliable result measurement norm was at E ≥2.53 eV, while the spectral range of the emission was within 380–495 nm and 570–750 nm. The incidence of bioelectrical activity of the body reducing the intensity of gas discharge glow. Pathology in the organism and surrounding tissues also alter the bioelectric activity and the shape and color of gas discharge glow. If the value is over than 2.54 eV this is an indicator of normal bioelectrical status. Some people with high energy status possess the values of photon emission over 2.90 eV. The high values of this parameter are possible with practicing of yoga, sport etc.

Fig. 9 shows the results of bioinfluencer Dimitar Risimanski with color coronal discharge. It illustrates, first, higher than normal level of biophoton emission from the thumb of the Bulgarian healer, and second, his ability to increase the patient's low biophoton emission. It is unfortunate that Ignatov & Mosin (2016) did not indicate whether the increased level of biophoton emission was permanent (which is unlikely given the data from Persinger's laboratory), and if it was increased before the healing session, then by what means?

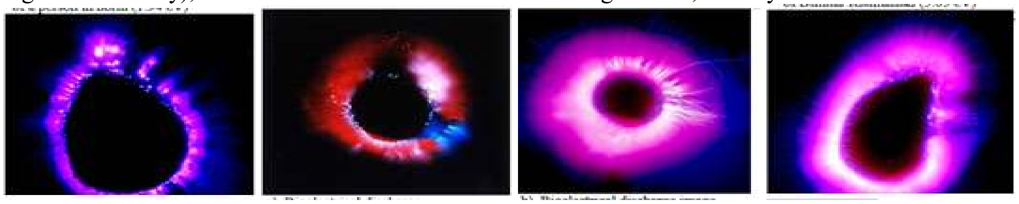

Discharge image in norm (2.64 eV) Low discharge image (1.94 eV) Risimanski image (3.03 eV) Image after healing (3.00 eV)

Fig. 9. Bioelectrical discharge images of the research with bioinfluencer Dimitar Risimanski (Ignatov & Mosin, 2016; *after our correction of the author's error*).

So, at least in three laboratories, using at least two methods, it has been documented that **mental exercises are accompanied by an increase in the emission of biophotons** from the surface of at least the **head and palms** of even ordinary people, not to mention meditators, psychics, and healers. Four separate experiments of the Persinger's laboratory documented concomitant **changes in EEG**, naturally quantitatively related to the emission of biophotons.

Rastmanesh & Pitkänen (2021), based on the studies we cited, wrot: hence one may argue that biophotons - or whatever is behind them - propagating along pathways parallel to axons analogous to wave guides could serve as carriers of neuronal and biological information. This would force the views about the role of nerve pulses to be challenged.

There is an extensive and at the same time contradictory literature on the effect of numerous meditation methods on the EEG (review: Faber et al., 2012), which we do not dwell on due to the lack of data on concomitant changes in biophoton emission. However, we recall the study of our favorite author (Newberg et al., 2001), in which the effect of meditation on brain activity was assessed by method of single photon emission computed tomography. In this study, authors presented SPECT data from eight practitioners of a form of Tibetan Buddhist meditation, performed specifically for spiritual, not-health-related, purposes. In this form of meditation, practitioners initially focus their attention on a **visualized image** and maintain that focus with increasing intensity. The 'peak' experience of their meditation is described as a sense of absorption into the **visualized image** associated with clarity of thought and a loss of the usual sense of space and time. The percentage change between meditation and baseline was compared. Significantly increased rCBF ($P<0.05$) was observed in the cingulate gyrus (prefrontal loci of EEG), inferior and orbital frontal cortex, dorsolateral prefrontal cortex (DLPFC), and thalamus. The change in rCBF in the left DLPFC correlated negatively ($P<0.05$) with that in the left superior parietal lobe.

It is time to move on to considering the original hypothesis of our "dual" colleagues Ohnishi & Ohnishi (2009; 2009a), who also embody a unique combination of a medicine doctor (a degree in biophysics) and a master of martial arts (a black belt in Aikido) as well as their branch the *Nishino Breathing Method* (NBM) that was developed by Master Nishino and called him the *Taiki-practice*. It is a method of enhancing the level of a students' Ki ("vitality" or "life-energy" as an important element in complementary and alternative medicine, CAM) through Ki-communication between an instructor and a student. When Nishino emits his Ki in the Taiki-practice, many of his students respond to it with various body movements (they jump, step back, run or roll on the floor). It has been known for 35 years that the practitioners of Ki experienced beneficial health effects. It was shown that the practice increased immune activity and decreased the stress level of the practitioners. From the collaboration with Master Nishino, Ohnishi & Ohnishi showed that 'Ki' is not a paranormal or parapsychological phenomenon, but a natural phenomenon. Using established biochemical and cellular models, authors demonstrated that Ki inhibited cultured cancer cell division (Ohnishi et al., 2005), it protected isolated rat liver mitochondria from oxidative injury (Ohnishi et al., 2006), and it may have a beneficial effect on osteoporosis (Ohnishi et al., 2007). Therefore, authors proposed that the healing effects of Ki may be related to (i) an **energy** aspect 'E' and (ii) an i**nformation** aspect (or an **entropy** aspect) 'S' of Ki (Ohnishi et al., 2006; Ohnishi, 2007).

Let's consider both aspects in more detail.

Ohnishi & Ohnishi observed that the propagation of Ki could be inhibited by a black vinyl curtain, a black acrylic plate, aluminum foil and a visible range optical filter (360–760 nm), but it was not inhibited by a near-infrared filter (800–2700 nm). Using a linear variable interference filter which can cover from 400 to 1100 nm, authors found that the Ki-energy had a peak around 1000 nm. Therefore, an **energy** aspect of **Ki** seems to be represented by **near-infrared radiation**. In order to build a model, authors analyzed various properties of Ki-energy by using the Taiki-reaction. In brief: Ohnishi ST emitted Ki toward a volunteer, and Ohnishi T measured the time between the start of emitting Ki and the time when the volunteer made a significant body motion. In other words, authors used a human being as a 'detector device' for Ki-energy. Ohnishi & Ohnishi used volunteers who can respond to his Ki with an unmistakable body motion (for example, fall down or run backward). Authors observed that the receiver's body moved both with and without the **blindfold**, indicating that the Taiki-reaction was caused by neither psychological nor hypnotic effects. The authors hypothesized that our bodies could **emit laser light**. The hypothesis is based on the fact that an essential secret in the practice of NBM is to keep the muscles of our bodies completely relaxed. If the emitter's hand is stiff, the Ki will not be released. Our skeletal muscle has a repeating striation of approximately 2500 nm, and the length of a thin filament (actin filament) is 1000 nm. If these repeating structures of skeletal muscle can cause a standing wave with a wavelength of 1000 nm, this can enhance the "laser" radiation. Therefore, skeletal muscle can serve as a "resonator of light". Unfortunately, further research into this possibility has not been conducted.

We specifically paid such great attention to the research of Ohnishi & Ohnishi, because their hypothesis about Ki as near-infrared radiation appeared at the same time, if not slightly earlier, then Bókkon's hypothesis about the emission of biophotons during mental exercise, which is fundamentally no different from Taiki-practice.

Ohnishi & Ohnishi (2006) note that in the Taiki-practice, the most interesting observation is that one can transfer **information** through Ki. An important concern in this five sense-independent communication is that the information is not a form of energy. It is a physical quantity called '**entropy**' as Shannon (1948) described it. Energy and entropy are two different physical quantities. The relationship between information and '**negative entropy**' in living cells was first pointed out by Schrödinger (1944), one of the key figures in the development of quantum physics. Of course living beings require energy for their growth, activity and reproduction. However, without information, they do not know how to grow, how to act and how to reproduce.

Ohnishi & Ohnishi (2006) cited the Shinagawa (1990) who discovered that a Qigong healer emitted information. His group found that the brain wave activity of a volunteer who sat down in front of a Qigong healer synchronized with that of the healer. He also observed that when the healer sent his Qi-energy, the subject lifted her hand. He was so surprised to see that information was dispatched by the healer, transmitted through the air and received by another individual. Actually, Shinagawa had witnessed a 'Taiki-effect.' Next authors cited the Machi (1993) who observed that infrared radiation (from 0.8 to 25 mm) was emitted from the hand of a Qigong healer, and that its amplitude was modulated with a low frequency of 1.2 Hz. He hypothesized that the information from the healer may be conveyed by the amplitude modulation of the infrared radiation. This is an interesting idea. However, if the information is carried by amplitude modulation of 1.2 Hz, then the time resolution of the information would be on the order of 1.2 s or longer. In the Nishino's Taiki-practice, his students respond to his instruction almost instantly. When Nishino sends signs to run or to stop, a student responds to it **immediately**, even though he/she was facing the opposite direction so that he/she could not see Nishino (observers can see both Nishino's gestures and student's responses). If it is not an amplitude modulation, then it may be either frequency modulation or digital modulation. Ohnishi & Ohnishi (2006) cite that in the past 30 years, many Chinese scientists regarded 'Qi' as a real substance flowing in our body, which can be represented by mass (m). On the contrary, most Japanese scientists treated 'Ki' as energy (E), except for Shinagawa who considered it to be information. The authors would like to propose that 'Qi' or 'Ki' has **both physical quantities of energy (E) and entropy (S)**. (According to Einstein, both E and m are the same physical entity, because $E=mc^2$).

It is time to demonstrate the ability of our colleague Dimitar Risimanski to influence the state of water.

Color Kirlian images of water droplets of different types of water are studied with Method of Color Coronal Spectral Analysis (Ignatov & Mosin, 2016). The photographing of the coronal spectrum is one of the physical methods in which the image has a much better quality on photographic film, than the electric images filmed with digital methods and with Polaroid. The dielectric permittivity of water is high and this is important for its properties as a solvent. Coronal images of waterdroplets show that different water perceives differently the electric field.

Fig. 10 shows the color coronal glow on photographic film of water drops from the control sample from deionized water (left) and deionized water after the bioinfluence of Dimitar Risimanski (right). The photon emission of the drop from the control sample is 2.07 eV. The photon emission of the drop from the sample is 2.71 eV. There is increasing of photon emission after the influence of Risimanski with 0.64 eV. Ignatov & Mosin (2016) concluded that this is the proof for increasing of electric permittivity as result of **restructuring** of water molecules after bioinfluence of Dimitar Risimanski. There are the following effects as results of restructuring of water molecules and reliable extremums in water spectrum - improvement of nervous conductivity, anti inflammatory effect, inhabitation of development of tumor cells of molecular level.

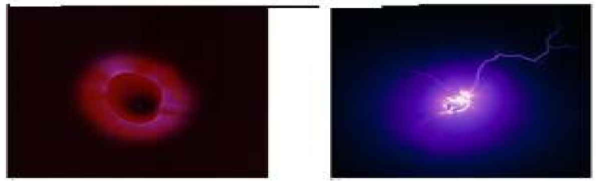

Fig. 10. Color coronal glow on photographic film of water drops from the control sample from deionized water (left) and deionized water after the bioinfluence of Dimitar Risimanski (right) (Ignatov & Mosin, 2016).

After citing the results of the experiment of Bulgarian colleagues conducted in 2016, it is time to present the results of the experiment conducted in 2013, the subject and at the same time the object of which was the first author of this article (Dobrovolsky et al., 2013). Valeriy Babelyuk, during the generation of KKK, directed his palms to an ampoule with factory distilled water. After the session, a specialist in physical optics, Dobrovolsky, DS, moistened a pellet of factory activated carbon with this water, placed it in a discharge-optical device designed and patented by him (Patent of Ukraine, 2010) and exposed it to three 7-10-second discharges (25 kV) from at an interval of 40 seconds, recording the brightness value in Cd/m^2 (Fig. 11). Distilled water from another ampoule of the same package served as a control.

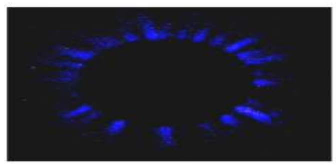

Fig. 11. A typical photographic image of the glow generated by a water-saturated activated carbon tablet (Dobrovolsky et al., 2013)

The KKK effect was evaluated by the ratio of the ***light activity*** of treated and ordinary distilled water. Three variants of the effect were found: enhancing, neutral and inhibitory (Fig. 12).

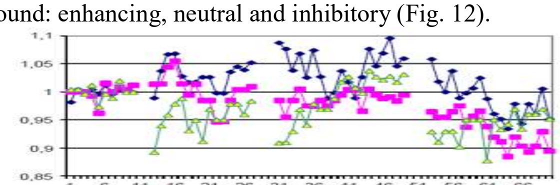

Fig. 12. Patterns of the ratio of light activity of water exposed to the influence of the Babelyuk to such without the influence (Dobrovolsky et al., 2013)

Being held captive by the academic demand for *reproducibility* of results, we judged this pilot experiment to be a failure. We were not aware that in the same 2013 Persinger et al. encountered a similar situation, so they further took into account the emission of biophotons only during the first 15 seconds after induction.

Nevertheless, on April 16, 2014 (on the eve of Easter), we dared to repeat the experiment, inviting our friend, the Greek Catholic priest Father Volodymyr, to take part in it in order to compare the effects of KKK and canonical Christian prayer of consecration of water to distilled water.

Alternate sequential effects on ampoules with distilled water gave the following series of changes (in percent) of its light activity (glow). KKK: 92; -3; 50; 143; Prayer: 224; -51; 4; 133. However, the another disappointment from the ambiguity of the data changed to heuristic delight after the analysis of the correlations between the changes in light activity of treated water and GDV parameters of both Operators after the sessions (Babelyuk et al., unpublished data, you will see in the next article). It turned out that both the directionality and the expressiveness of the influence on the light activity of water of both mental practices are determined by the state of the third chakra of the operators (Fig. 13).

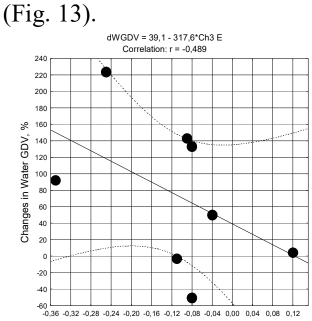

Fig. 13. Scatterplot of correlation between Karate Master's and Greek-Katholic Priest's third Chakra Energy during Katas or Prayer (X-line) and changes in the light activity of water they treated (Y-line)

It is interesting that Father Volodymyr was not at all surprised by the ineffectiveness of the second and third Prayers, informing us that according to the canons, priests are allowed to consecrate water only once a day!

Thus, there are good reasons to assume that **KKK causes a significant increase in the electrical activity and negentropy of neurons in individual structures of Babelyuk's brain, which is accompanied by an increase in the emission of biophotons by neurons and their negentropy**. According to Pessinger's laboratory, biophotons, penetrating through the bones and scalp, fall into distilled water placed in front of the operator. However, referring to the experiments of Rubik & Jabs (2017), we consider the situation more realistic that **brain biophotons are transferred through the meridians to the acupuncture points of the fingers and from there into the water**.

Both Valeriy Babelyuk and Dimitar Risimanski as well as Father Volodymyr through mental practices are able to change light activity of water.

However, the statement of increased energy levels and the cluster formations of water treated by mental practices still does not explain how this water transmits information from Babelyuk's brain to the brains of recipients who drank this water, and **blindly**, that is, in the absence of a **placebo effect**.

So, let's move on to the apotheosis of the discussion - the concept of “water memory” with its bright appearance, subsequent discrediting and even trolling, but triumphant revival (Davenas, … & Benveniste, 1988; Benveniste, 2005; Beauvais, 2024). Benveniste’s results have now been confirmed in multiple laboratories (Jerman et al., 2005; Montagnier et al., 2009; 2011; 2015; 2017; Pollack, 2013; Kroeplin & Henschel, 2016; Chang et al., 2019; Tang et al., 2019).

Numerous publications from Montagnier’s lab have measured low-frequency EM signals from DNA in serially diluted solutions after activation by exogenous electromagnetic (EM) fields. These EM signals can be measured and stored using conventional EM detectors. In addition, these EM signals can be transferred via a resonance phenomenon to separate aqueous solutions and can induce the formation of water nanostructures which serve as a DNA template to recreate the intact original DNA (Montagnier et al., 2009; 2015). A mechanism for the recreation of DNA using water nanostructures has been proposed where the Taq-DNA polymerase enzyme can apparently “see” the EM signature of the DNA by exchanging wave fields. Such a mechanism is consistent with the gauge theory paradigm of quantum field theory (Kurian et al., 2018; Montagnier et al., 2017).

A new impetus for the development of the concept was the discovery of water’s fourth phase, otherwise known as “EZ (exclusion zones) water” (Pollack, 2013; 2022). EZ (otherwise known as “fourth-phase”) water may behave much like a computer memory, capable of storing biological information. Along with the notion of information acquisition comes evidence that EZ water may be impacted by subtle energies. Long known but only recently coming under serious study, those energies can demonstrably influence water. The impacted water is presumably its EZ fraction, whose crystal-like structure allows for information-storage capability. Ordinary liquid water has no such capability: its randomly oriented, rapidly fluctuating molecules would be expected to show no capacity for retention of information. EZ water, on the other hand, seems practically “designed” to carry information.

Pollack (2022) suggest that the EZ water may be susceptible to external influence, and here he refer to the so-called “subtle energies” or “biofields”, which may come from outside. Regarding our experiment, such an external influence on water could be the flow of biophotons from the acupuncture points of the fingers extended above the vessel in which this water is located, and also, less likely, the head.

Unlike the cited experiments, in our experiment, firstly, information was transferred to the water not about the operator's DNA, but about the electrical activity of the neurons in his brain; secondly, to transfer such information it was not necessary to use water activation by exogenous electromagnetic fields. When consumed by recipients, this water, as a carrier of energy and information, somehow affects at least their neurons, as documented by changes in EEG. It seems quite likely that the treated water also affects immunocytes and endocrinocytes, both directly and through neurons within the triune neuro-endocrine-immune complex. In the following articles we will demonstrate that the KKK session causes an increase in synaptic efficacy of rat hippocampal slice as well as changes in GDV, EEG, HRV and immune parameters of volunteers.

The research tested three main hypotheses regarding the neurotropic effects of Kyokushin Karate Katas (KKK)-treated water. Analysis of the results provides the following verification.

Hypothesis 1, **which postulated that distilled water exposed to KKK induces significant and measurable neurotropic effects distinct from control waters, was confirmed** through discriminant analysis (Wilks' $\Lambda=0.214$; $\chi^2_{(50)}=116$; $p<10^{-6}$). The classification accuracy reached 95.6% overall, with 100% accuracy for KKK-treated water group. The Mahalanobis distances showed significant separation between KKK-treated water and both baseline ($D^2=15.7$; $F=2.13$; $p=0.008$) and control waters ($D^2=25.6$; $F=2.79$; $p=0.001$).

Hypothesis 2, **regarding biophotonic resonance impact on neurophysiological activity, was partially confirmed.** Significant effects were documented on EEG parameters, including enhancement of δ-rhythm in F8 locus ($Z=0.81$) and α-rhythm index ($Z=0.78$), as well as inhibitory effects on θ-rhythm PSD across multiple loci (mean $Z=-0.53\pm0.09$; $p<0.01$). HRV parameters showed significant modulation, including heart rate ($Z=-0.39$)

and 1/Mode HRV (Z=-0.27). However, while the neurophysiological effects were statistically significant, the direct mechanism of biophotonic resonance transfer remains theoretical rather than empirically proven.

Hypothesis 3, concerning individual variation in response magnitude, was confirmed through analysis of individual response patterns. The study identified distinct responder categories (3 moderate and 2 severe), with participants Ly and Kh demonstrating maximum sensitivity to KKK-treated water effects.

These findings were derived through robust statistical methodology including discriminant analysis, ANOVA, classification accuracy testing, Mahalanobis distance calculations, Z-score normalizations, and entropy analysis.

The strongest statistical support exists for Hypothesis 1, with comprehensive multivariate analysis demonstrating clear differentiation of KKK-treated water effects. While Hypothesis 2 is partially supported by significant neurophysiological changes, the mechanistic aspects require further validation. Hypothesis 3 is well-supported by individual response data, though the limited sample size (n=5) suggests the need for larger-scale validation studies.

Conclusions.

1. The neurotropic effect of Kyokushin Karate Katas (KKK)-treated water has been conclusively demonstrated through discriminant analysis (Wilks' Λ=0.214; $\chi^2_{(50)}$=116; $p<10^{-6}$), with 95.6% classification accuracy and perfect discrimination of the KKK-treated water group (100% accuracy).
2. Three distinct patterns of neurotropic effects were identified.

a) In the absence of spontaneous rhythmic changes (Z±SD = 0.02±0.12), enhancing effects were observed on: δ-rhythm PSD in F8 locus (Z=0.81); α-rhythm index (Z=0.78); Right-side shift in θ-rhythm laterality (Z=0.37) Average effect magnitude: Z=0.65±0.25.

b) Against weak inhibitory spontaneous changes (Z=-0.22±0.15), pronounced inhibitory effects were found on: θ-rhythm PSD across multiple loci (P3: Z=-0.55; C4: Z=-0.54; T3: Z=-0.50); Entropy of PSD (C4: Z=-0.77; P3: Z=-0.55; F4: Z=-0.47). ULF band HRV (Z=-0.55) Average effect magnitude: Z=-0.53±0.09.

c) Against enhancing spontaneous changes (Z=0.35±0.17), essential inhibitory effects were found on: θ-rhythm frequency (Z=-1.40). θ-rhythm PSD in T5 (Z=-0.84); α-rhythm PSD in F8 (Z=-0.70); Heart rate (Z=-0.39) Average effect magnitude: Z=-0.63±0.40.

3. Significant individual variations in response were documented (F=3.82; $p<10^{-5}$), with participants categorized as moderate (n=3) or severe (n=2) responders. The Mahalanobis distances confirmed distinct separation between individual response patterns (D^2=15.7-25.6; p<0.01).
4. The information transfer mechanism demonstrates high specificity, as evidenced by the discriminant function analysis (r*=0.779 for the first root, accounting for 64.7% of the variance; r*=0.676 for the second root, accounting for 35.3% of variance).
5. These conclusions are supported by comprehensive statistical analysis, including multivariate discriminant analysis, entropy calculations, and normalized effect size measurements. The findings demonstrate robust and reproducible neurotropic effects of KKK-treated water, though the exact mechanism of information transfer requires further investigation. The study's limitations include the relatively small sample size (n=5), suggesting the need for larger-scale validation studies. The statistical significance and effect sizes observed provide strong evidence for the reality of the documented phenomena. These findings have important implications for understanding bioenergetic information transfer and its effects on neurophysiological parameters, opening new avenues for research in biofield science and consciousness studies.

Acknowledgment

We express sincere gratitude to employees of clinical sanatorium "Moldova" (Truskavets') for help in carry out of tests. Special thanks to the volunteers.

We dedicate the article to the 150th anniversary of the Ukrainian-Jewish luminary Oleksandr Gurwitsch (October 9, 1874, Poltava - July 27, 1954, Moscow), nominated for the Nobel Prize in Physiology and Medicine in 1929, 1932-1934, 1938, but removed from science after the infamous VASKhNIL 1948 session.

Accordance to ethics standards

Tests in patients are carried out in accordance with positions of Helsinki Declaration 1975, revised and complemented in 2002, and directive of National Committee on ethics of scientific researches. During realization of tests from all participants the informed consent is got and used all measures for providing of anonymity of participants.

References

Babelyuk, V. E., Popovych, I. L., & Zukow, W. (2024). Neurotropic effects of distilled water administered to recipients under the guise of exposure to Kyokushin karate katas. *Journal of Physical Education and Sport*, 24(11), 1490-1509. https://doi.org/10.7752/jpes.2024.11276

Baevsky, R., & Chernikova, A. (2017). Heart rate variability analysis: physiological foundations and main methods. *Cardiometry*, 10, 66-76. https://doi.org/10.12710/CARDIOMETRY.2017.10.6676

Baevsky, R. M., & Ivanov, G. G. (2001). Heart rate variability: Theoretical aspects and possibilities of clinical application. *Medicine of the Russian Federation*, 8, 6-12.

Beauvais, F. (2024). Benveniste's experiments and the so-called "water memory" phenomenon: An example of serendipity? *Investigation and Experiments Hypothesis*.

Beloussov, L. V., Opitz, J. M., & Gilbert, S. F. (1997). Life of Alexander G. Gurwitsch and his relevant contribution to the theory of morphogenetic fields. *International Journal of Developmental Biology*, 41(6), 771-777.

Benveniste, J. (2005). *Ma vérité sur la mémoire de l'eau*. Albin Michel.

Berntson, G., Bigger, J. T., Eckberg, D. L., Grossman, P., Kaufmann, P. G., Malik, M., Nagaraja, H. N., Porges, S. W., Saul, J. P., Stone, P. H., & Van Der Molen, M. W. (1997). Heart rate variability: Origins, methods, and interpretive caveats. *Psychophysiology*, 34(6), 623-648. https://doi.org/10.1111/j.1469-8986.1997.tb02140.x

Chang, B. Q., Li, T., Bai, X., Zhao, M., Wang, B., Rein, G., & Chen, Y. (2019). Rate limiting factors for DNA transduction induced by weak electromagnetic field. *Electromagnetic Biology and Medicine*, 38(1), 55-65. https://doi.org/10.1080/15368378.2019.1566451

Cohen, S., & Popp, F. A. (1997). Biophoton emission of human body. *Journal of Photochemistry and Photobiology B: Biology*, 40(2), 187-189. https://doi.org/10.1016/S1011-1344(97)00050-X

Davenas, E., Beauvais, F., Amara, J., Oberbaum, M., Robinzon, B., Miadonnai, A., ... & Benveniste, J. (1988). Human basophil degranulation triggered by very dilute antiserum against IgE. *Nature*, 333(6176), 816-818. https://doi.org/10.1038/333816a0

Dobrovolskyi, Y. G., Gozhenko, A. I., Babelyuk, V. E., & Popovych, I. L. (2013). Methodology for studying the structure of water using a discharge-optical device and demonstration of the possibility of energy-informational influence on it by the operator [in Ukrainian]. *Water: Hygiene and Ecology*, 2(1), 120-135.

Dotta, B. T., Saroka, K. S., & Persinger, M. A. (2012). Increased photon emission from the head while imagining light in the dark is correlated with changes in electroencephalographic power: Support for Bókkon's biophoton hypothesis. *Neuroscience Letters*, 513(2), 151-154. https://doi.org/10.1016/j.neulet.2012.02.021

Gozhenko, A., Korda, M., Popadynets', O., & Popovych, I. (2021). *Entropy, Harmony, Synchronization and their Neuro-endocrine-immune Correlates*. Odesa: Feniks.

Gurwitsch, A. G. (1926). Das Problem der Zellteilung physiologisch betrachtet. In *Das Problem der Zellteilung Physiologisch Betrachtet* (pp. 473-475). Springer.

Gurwitsch, A. G. (1945). *Theory of biological field*. Soviet Science.

Gurwitsch, A. G. (1959). *Die mitogenetische Strahlung, ihre physikalisch-chemischen Grundlagen und ihre Anwendung in Biologie und Medizin*. Fischer.

Heart Rate Variability Task Force. (1996). Heart rate variability: Standards of measurement, physiological interpretation, and clinical use. *Circulation*, 93(5), 1043-1065. https://doi.org/10.1161/01.CIR.93.5.1043

Hunter, M. D., Dotta, B. T., Saroka, K. S., Lavallee, C. F., Koren, S. A., & Persinger, M. A. (2010). Cerebral dynamics and discrete energy changes in the personal physical environment during intuitive-like states and perceptions. *Journal of Consciousness Exploration & Research*, 1(9), 1179-1197.

Ignatov, I., & Mosin, O. V. (2016). Color coronal spectral analysis for modeling of nonequilibrium conditions with the gas electric discharge, simulating primary atmosphere. *European Journal of Molecular Biotechnology*, 11(1), 12-33.

Jerman, I., Ružič, R., Krašovec, R., Škarja, M., & Mogilnicki, L. (2005). Electrical transfer of molecule information into water, its storage, and bioeffects on plants and bacteria. *Electromagnetic Biology and Medicine*, 24(3), 341-353. https://doi.org/10.1080/15368370500379574

Kataoka, Y., Cui, Y., Yamagata, A., Niigaki, M., Hirohata, T., Oishi, N., & Watanabe, Y. (2001). Activity-dependent neural tissue oxidation emits intrinsic ultraweak photons. *Biochemical and Biophysical Research Communications*, 285(4), 1007-1011. https://doi.org/10.1006/bbrc.2001.5285

Kirlian, S. D. (1949). Method for receiving photographic pictures of different types of objects. Patent №106401.

Kirlian, S. D., & Kirlian, V. K. (1961). Photography and visual observation by means of high-frequency currents. *Journal of Scientific and Applied Photography*, 6(6), 397-403.

Klecka, W. R. (1989). Discriminant analysis [trans. from English in Russian]. In *Factor, Discriminant and Cluster Analysis* (pp. 78-138). Finansy i Statistika.

Kobayashi, M., Takeda, M., Ito, K. I., Kato, H., & Inaba, H. (1999). Two-dimensional photon counting imaging and spatiotemporal characterization of ultraweak photon emission from a rat's brain in vivo. *Journal of Neuroscience Methods*, 93(2), 163-168. https://doi.org/10.1016/S0165-0270(99)00140-5

Kobayashi, M., Takeda, M., Sato, T., Yamazaki, Y., Kaneko, K., Ito, K., ... & Inaba, H. (1999a). In vivo imaging of spontaneous ultraweak photon emission from a rat's brain correlated with cerebral energy metabolism and oxidative stress. *Neuroscience Research*, 34(2), 103-113. https://doi.org/10.1016/S0168-0102(99)00040-1

Koenig, H. L., Krueger, A. P., Lang, S., & Sonning, W. (1981). *Biologic effects of environmental electromagnetism*. Springer Science & Business Media.

Kroeplin, B., & Henschel, R. C. (2016). *World in a Drop: Memory and Consciousness in Water*. Crotona.

Kurian, P., Dunston, G. A., & Lindesay, J. (2018). DNA in a quantum superposition? On the influence of enzymatic conformational fluctuations on quantum coherence lifetimes of drug-DNA intercalation. *Journal of Theoretical Biology*, 452, 47-55. https://doi.org/10.1016/j.jtbi.2018.05.012

Machi, Y. (1993). The science of Ki. *Osaka Research Institute of Life Physics*, 16, 15-22.

Montagnier, L., Aissa, J., Ferris, S., Montagnier, J. L., & Lavallee, C. (2009). Electromagnetic signals are produced by aqueous nanostructures derived from bacterial DNA sequences. *Interdisciplinary Sciences: Computational Life Sciences*, 1, 81-90. https://doi.org/10.1007/s12539-009-0036-7

Montagnier, L., Aïssa, J., Del Giudice, E., Lavallee, C., Tedeschi, A., & Vitiello, G. (2011). DNA waves and water. *Journal of Physics: Conference Series*, 306, 012007. https://doi.org/10.1088/1742-6596/306/1/012007

Montagnier, L., Del Giudice, E., Aïssa, J., Lavallee, C., Motschwiller, S., Capolupo, A., ... & Vitiello, G. (2015). Transduction of DNA information through water and electromagnetic waves. *Electromagnetic Biology and Medicine*, 34(2), 106-112. https://doi.org/10.3109/15368378.2015.1036072

Montagnier, L., Aïssa, J., Capolupo, A., Craddock, T. J., Kurian, P., Lavallee, C., ... & Vitiello, G. (2017). Water bridging dynamics of polymerase chain reaction in the gauge theory paradigm of quantum fields. *Water*, 9(5), 339. https://doi.org/10.3390/w9050339

Newberg, A. B., Alavi, A., Baime, M., Pourdehnad, M., Santanna, J., & d'Aquili, E. (2001). The measurement of regional cerebral blood flow during the complex cognitive task of meditation: A preliminary SPECT study. *Psychiatry Research: Neuroimaging*, 106(2), 113-122. https://doi.org/10.1016/S0925-4927(01)00074-9

Ohnishi, S. T., & Ohnishi, T. (2009). Philosophy, psychology, physics and practice of Ki. *Evidence-Based Complementary and Alternative Medicine*, 6(2), 175-183. https://doi.org/10.1093/ecam/nen073

Ohnishi, S. T., & Ohnishi, T. (2009a). How far can Ki-energy reach? A hypothetical mechanism for the generation and transmission of Ki-energy. *Evidence-Based Complementary and Alternative Medicine*, 6(3), 379-391. https://doi.org/10.1093/ecam/nem102

Ohnishi, T., Ohnishi, S. T., Nishino, K., Tsurusaki, Y., & Yamaguchi, M. (2005). Growth inhibition of cultured cancer cell lines by Ki-energy (life-energy). *Evidence-Based Complementary and Alternative Medicine*, 2(3), 387-393. https://doi.org/10.1093/ecam/neh116

Ohnishi, S. T., Ohnishi, T., & Nishino, K. (2006). Ki-energy (life-energy) protects isolated mitochondria from oxidative injury. *Evidence-Based Complementary and Alternative Medicine*, 3(4), 475-482. https://doi.org/10.1093/ecam/nel027

Ohnishi, S. T., Nishino, K., Uchiyama, K., Ohnishi, T., & Yamaguchi, M. (2007). Ki-energy (life-energy) stimulates osteoblastic cells and inhibits the formation of osteoclast-like cells in bone cell culture models. *Evidence-Based Complementary and Alternative Medicine*, 4(2), 225-232. https://doi.org/10.1093/ecam/nel077

Persinger, M. A. (2010). 10−20 Joules as a neuromolecular quantum in medicinal chemistry: An alternative approach to myriad molecular pathways? *Current Medicinal Chemistry*, 17(27), 3094-3098. https://doi.org/10.2174/092986710791959701

Persinger, M. A., Dotta, B. T., Saroka, K. S., & Scott, M. A. (2013). Congruence of energies for cerebral photon emissions, quantitative EEG activities and ~5 nT changes in the proximal geomagnetic field support spin-based hypothesis of consciousness. *Journal of Consciousness Exploration & Research*, 4(1), 1-24.

Polovynko, I. S., Zayats, M. V., Zukow, W., Popovych, I. L. (2016). Neuro-endocrine-immune relationships by chronic stress at male rats. *Journal of Health Sciences*, 6(12), 197-214.

Pollack, G. H. (2013). *The fourth phase of water: Beyond solid, liquid, and vapor*. Ebner and Sons.

Pollack, G. H. (2022). EZ Water and the Origin of Life. *Annual Research & Review in Biology*, 37(9), 18-28. https://doi.org/10.9734/arrb/2022/v37i930600

Popadynets', O., Gozhenko, A., Zukow, W., & Popovych, I. (2020). Relationships between the entropies of EEG, HRV and immunity. *Journal of Physical Education and Sport*, 20(3), 1554-1564. https://doi.org/10.7752/jpes.2020.03214

Popp, F. A., Nagl, W., Li, K. H., Scholz, W., Weingärtner, O., & Wolf, R. (1984). Biophoton emission: New evidence for coherence and DNA as source. *Cell Biophysics*, 6(1), 33-52. https://doi.org/10.1007/BF02788579

Rahnama, M., Tuszynski, J. A., Bókkon, I., Cifra, M., Sardar, P., & Salari, V. (2011). Emission of mitochondrial biophotons and their effect on electrical activity of membrane via microtubules. *Journal of Integrative Neuroscience*, 10(1), 65-88. https://doi.org/10.1142/S0219635211002622

Rastmanesh, R., & Pitkänen, M. (2021). Can the Brain Be Relativistic? *Frontiers in Neuroscience*, 15, 659860. https://doi.org/10.3389/fnins.2021.659860

Rubik, B., & Jabs, H. (2017). Effects of intention, energy healing, and mind-body states on biophoton emission. *Cosmos and History: The Journal of Natural and Social Philosophy*, 13(2), 227-247.

Saroka, K. S., Dotta, B. T., & Persinger, M. A. (2013). Concurrent photon emission, changes in quantitative brain activity over the right hemisphere, and alterations in the proximal geomagnetic field while imagining white light. *International Journal of Life Science and Medical Research*, 3(1), 30-34.

Schrödinger, E. (1944). *What is Life? - The Physical Aspect of the Living Cell*. Cambridge University Press.

Shannon, C. E. (1948). A mathematical theory of information. *Bell System Technical Journal*, 27, 379-423.

Shinagawa, Y. (1990). The science of Qigong. *Tokyo Denki University Press*.

Tang, B. Q., Li, T., Bai, X., Zhao, M., Wang, B., Rein, G., & Chen, Y. (2019). Rate limiting factors for DNA transduction induced by weak electromagnetic field. *Electromagnetic Biology and Medicine*, 38(1), 55-65. https://doi.org/10.1080/15368378.2019.1566451

Van Wijk, R., Bosman, S., Ackerman, J., & Van Wijk, E. (2008). Correlation between fluctuations in human ultra-weak photon emission and EEG alpha rhythm. *NeuroQuantology*, 6(4), 452-463.

Van Wijk, R., Van Wijk, E. P., & Bajpai, R. P. (2006). Photocount distributions of photons emitted from three sites of the body. *Journal of Photochemistry and Photobiology B: Biology*, 84(1), 46-55. https://doi.org/10.1016/j.jphotobiol.2006.01.010

Wiener, N. (1954). *The Human Use of Human Beings*. Houghton-Mifflin.

Zukow, W., Muszkieta, R., Hagner-Derengowska, M., Kułakowska, D., Kułakowski, P., Ostrowska, B., Gozhenko, A. I., & Popovych, I. L. (2022). Effects of rehabilitation at the Truskavets' spa on physical working capacity and its neural, metabolic, and hemato-immune accompaniments. *Journal of Physical Education and Sport*, 22(11), 2708-2722. https://doi.org/10.7752/jpes.2022.11345